SCIENTIFIC REPORTS

OPEN

SUBJECT AREAS:
CHEMICAL ENGINEERING
SYNTHESIS AND PROCESSING

Received
13 September 2013

Accepted
4 December 2013

Published
6 January 2014

Correspondence and requests for materials should be addressed to H.H. (hh1001@hanyang.ac.kr); S.S.K. (sangsub@inha.ac.kr) or H.W.K. (hyounwoo@hanyang.ac.kr)

Evidence of Ostwald ripening during evolution of micro-scale solid carbon spheres

Heon Ham[1], No-Hyung Park[2], Sang Sub Kim[3] & Hyoun Woo Kim[4]

[1]H&H Co. Ltd., Korea National University of Transportation, 50 Daehak-ro, Chungju-si, Chungbuk 330-702, Republic of Korea, [2]Department of Textile Convergence of Biotechnology & Nanotechnology, Korea Institute of Industrial Technology 1271-18 Sa 3-dong, Sangnok-gu, Ansan-si, Gyeonggi-do, 426-910, Republic of Korea, [3]Department of Materials Science and Engineering, Inha University, Incheon 402-751, Republic of Korea, [4]Division of Materials Science and Engineering, Hanyang University, Seoul 133-791, Republic of Korea.

Ostwald ripening is an evolutionary mechanism that results in micro-scale carbon spheres from nano-scale spheres. Vapor-phase carbon elements from small carbon nanoparticles are transported to the surface of submicron-scale carbon spheres, eventually leading to their evolution to micro-scale spheres via well-known growth mechanisms, including the layer-by-layer, island, and mixed growth modes. The results obtained from this work will pave the way to the disclosure of the evolutionary mechanism of micro-scale carbon spheres and open a new avenue for practical applications.

The coarsening of nanoparticles occurs through two fundamentally different mechanisms[1–3]: In one mechanism, which is known as coalescence, the crystal sphere grows from migration and coalescence of islands or particles over the substrate surface[3,4]. The other mechanism, which is known as Ostwald ripening[5–8], is related to the growth by interparticle transport of single atoms[3], in which larger particles grow at the expense of smaller particles[9]. Its driving force is the difference in chemical potential, which arises from the difference in the radius of the curvature of the droplets or particles[8].

Carbon spheres have been intensively studied because of their peculiar properties and promising applications. Carbon spheres can be classified by two groups: hollow spheres and solid spheres. Most research has focused on the synthesis of hollow carbon spheres owing to their promising applications in drug delivery, encapsulation, and protection of biological-active agents[10–12]. However, in spite of the great potential in lubricating materials, gas storage media, and catalyst supports[13–15], the synthesis of solid carbon spheres (SCSs) has rarely been reported. In particular, it is imperative to reveal which mechanism mainly dominates in the evolution of SCSs between the two cited mechanisms: coalescence and Ostwald ripening.

In this paper, micro-scale SCSs were synthesized using the microwave method. As an inexpensive, quick, and versatile technique, microwave can heat the carbon materials to a high temperature in a short time[16]. Accordingly, a variety of nanostructures have been fabricated via the energy efficient microwave irradiation approach[17–20]. In our study, the graphene oxide (GO) was put onto an alumina boat, which was heated in a microwave oven for three minutes, and the growth mechanism of the micro-scale SCSs were investigated by transmission electron microscopy (TEM), selected area electron diffraction (SAED) pattern, field emission scanning electron microscopy (FE-SEM), and Raman spectroscopy. This study revealed that the evolution of micro-scale SCSs is mainly controlled by the Ostwald-ripening process. In regard to the composite scheme with micro- or nano-scale carbon materials, the Ostwald ripening played a significant role in the growth phenomena. For example, it played a role in the growth of catalytic particles in a single-walled carbon nanotube (CNT) forest[21,22], in the electrochemical growth of metal catalysts supported on carbon[23], and in the growth of metal clusters attached to CNTs[24]. In addition, the effects of Ostwald ripening of catalytic particles on CNT chirality distributions were investigated[25]. However, to our best knowledge, there has been no report on the Ostwald-ripening growth of carbon nanomaterial itself, including SCSs.

Results

Figure 1 shows FE-SEM images of the formation of micro-scale SCSs. Figure 1a shows that both nano-scale and micro-scale SCSs formed on the GO surface. Figure 1b indicates that nano-scale SCSs with a diameter of less than

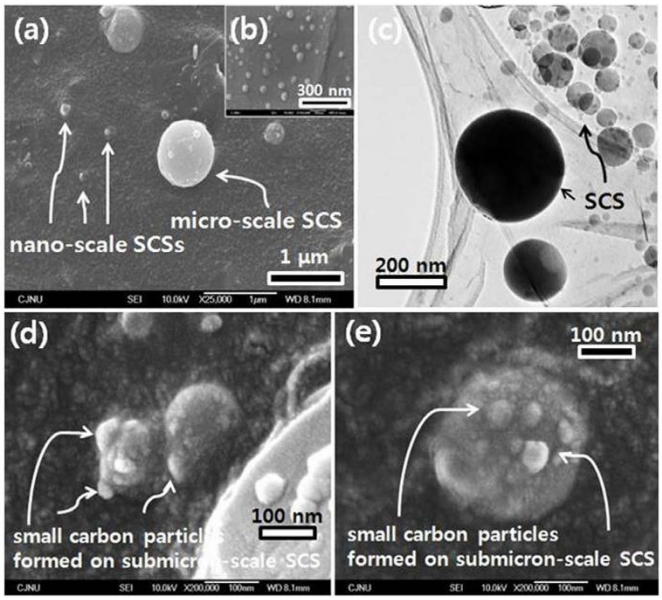

Figure 1 | Microstructures of micro-scale and nano-scale SCSs. (a) FE-SEM image of micro-scale and nano-scale SCSs on GO. (b) FE-SEM image of nano-meter sized SCSs. (c) TEM image of SCSs. (d) Side-view and (e) top-view images exhibiting the attachment of nano-scale particles to the surface of submicron-scale SCSs.

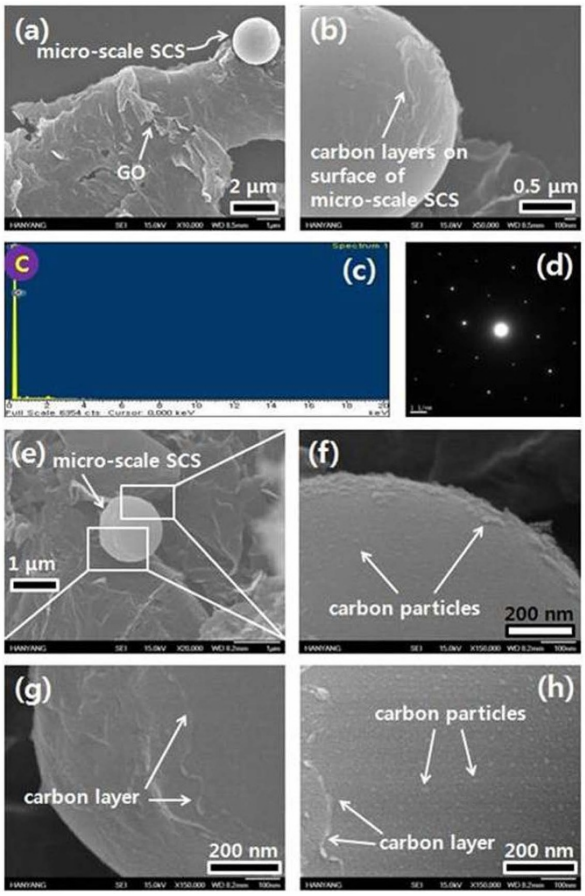

Figure 2 | Observation of surface of micro-scale SCSs. (a) FE-SEM image of a micro-scale SCS. (b) Enlarged image of the surface of the micro-meter-sized carbon sphere in (a). (c) EDX and (d) SAED spectrum of the micro-scale SCS. (e) FE-SEM image of a micro-scale SCS. (f–h) Enlarged images of the micro-scale SCS in (e).

10 nm formed on the GO sheet. Because nano-scale SCSs act as a seed of micro-scale SCSs, we investigated the detailed growth process of nano-scale SCSs by TEM images. Figure 1c shows the formation of SCSs of various sizes on GO. In this case, it is very likely that nano-scale SCSs coarsened by interacting with other SCSs in the crowded area. Figure 1d shows a side-view image that exhibits the attachment of nano-scale particles to the surface of neighboring SCSs. Subsequently, small SCSs become larger by means of the diffusion/transport of carbon atoms from neighboring small SCSs. Figure 1e shows a top-view image, which indicates that some particles formed on the surface of much larger-diameter SCSs.

With Figure 1, we can explain the associated growth mechanisms as follows. In the beginning, nano-scale SCSs nucleate on the surface of GO. At this stage, small and large SCSs exist simultaneously (Figures 1a–1c). Subsequently, small carbon nuclei grow larger by the attachment of carbon particles on the surface of other ones (Figures 1d, 1e). However, it is not clear whether or not the attachment of carbon particles was operated by Ostwald ripening. One possibility is that small particles can be attached to the larger ones by the coalescence mechanism. The other possibility is that the small particles are nucleated on the surface of the larger particles, presumably by the vapor transport of carbon atoms; this process is operated by the island growth based on the Ostwald ripening. In this case, the diameter of SCSs increases by the attachment of small carbon particles to the surface. The surface of larger-sized SCSs acts as a substrate for the subsequent deposition of smaller-sized carbon particles, as shown in Figure 1e. Larger-sized SCSs were investigated in detail in the following figures.

Figure 2a shows an FE-SEM image of a micro-scale SCS, which was grown on GO. Figure 2b shows an enlarged image of the micro-scale SCS in Figure 2a. It is noteworthy that, overall, there are uniform layers on the surface of the micro-scale SCS. The formation of a carbon layer is likely to be associated with the surface diffusion of carbon atoms on the surface of a micro-scale SCS, following the layer-by-layer growth mode (i.e., the Franck-van der Merwe growth mechanism). Figure 2c shows an energy dispersive X-ray spectroscopy spectrum of the micro-scale SCS of Figure 2a (C = 97 wt%, O = 3 wt%). The SAED pattern of the micro-scale SCS corresponds to that of pristine graphite (Figure 2d)).

We investigated another micro-scale SCS by FE-SEM, as shown in Figure 2e. Figures 2f–2h correspond to enlarged images of the micro-scale SCS in Figure 2e. In Figure 2f, it is evident that nano-scale carbon particles cover the surface of the micro-scale SCS, being associated with the island mode (i.e., the Volmer-Weber growth mechanism). Figure 2g exhibits the formation of a layered structure on the surface of a micro-scale SCS. Here, the carbon layer formed in the course of the diffusion of carbon atoms on the surface of the micro-scale SCS, exhibiting the layer-by-layer growth mode. In Figure 2h, very tiny carbon particles formed on the layer-like structure, which resides on the surface of the micro-scale SCS.

In this case, we surmise that carbon atoms diffused onto the surface of micro-scale SCSs to generate a layered structure. Simultaneously, very tiny carbon particles formed on the carbon layer. Accordingly, the associated growth mechanism is likely to be linked with the mixed mode (i.e., the Stranski-Krastanov growth mechanism). Figure 2 indicates that the micro-scale SCS grows by the island, the layer-by-layer, and the mixed modes, which are associated with vapor deposition behavior. This reveals that the overall growth of micro-scale SCSs takes place on the basis of Ostwald ripening.

We investigated the growth of carbon particles on the larger (micro-scale) SCSs by FE-SEM, as shown in Figure 3. Figure 3a shows an SEM image of a micro-scale SCS. Figures 3b–3d represent the surface views of the micro-scale SCS in Figure 3a. In Figure 3b, an island-like nanostructure with a diameter of about 80 nm is

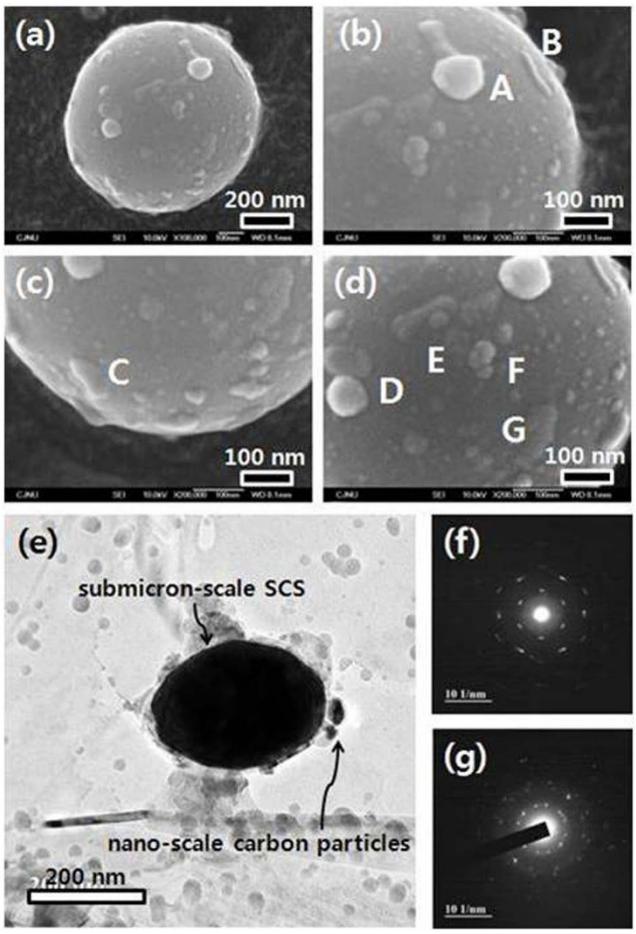

Figure 3 | Formation of carbon particles on micro-scale SCS. (a) FE-SEM image of a micro-scale SCS. (b–d) Enlarged images of a micro-scale SCS in (a). (e) TEM image of small carbon particles being attached to a submicro-scale SCS. (f, g) SAED spectra of (f) submicron-scale SCS and (g) nano-scal carbon particle.

designated as "A". "B" shows a coarsening image of a carbon particle with a line-like morphology. "C" in Figure 3c also exhibits growth behavior of the SCS by the formation of an island-like nanostructure. In Figure 3d, the carbon island is shown in "D". It is of note that the growth of the SCS is dominated by the island growth mode. In "E", small carbon islands are created on the relatively flat islands. Accordingly, the growth observed in "E" mainly follows the island mode, with a mixed mode (i.e., the Stranski-Krastanov growth mechanism) being incorporated. It is noteworthy that "F" shows that small carbon particles happen to be deposited on the large one. Although the structures in "G" exhibit a layer-like morphology, we surmise that the related growth is closer to the island mode.

We investigated the growth of SCSs in more detail, by means of TEM investigation. Figure 3e shows a typical TEM image of an SCS, which was generated on GO. Around the submicron-scale SCS, a number of nano-scale particles are attached. The SAED pattern of large sized carbon particles obviously shows the graphite structure in Figure 3f, but the SAED pattern of nano-scale particles corresponds to a turbostratic carbon structure, which is shown in Figure 3g. This indicates that the carbon particles were generated directly from the vapor phase in a non-equilibrium manner. The TEM analysis indicates that the attached carbon particles are in their disordered state, excluding the possibility of growth by coalescence, in which two ordered graphitic particles agglomerate. Accordingly, the SCS grows by the island and mixed modes, which are associated with vapor deposition behavior. That is, carbon atoms diffuse onto the surface

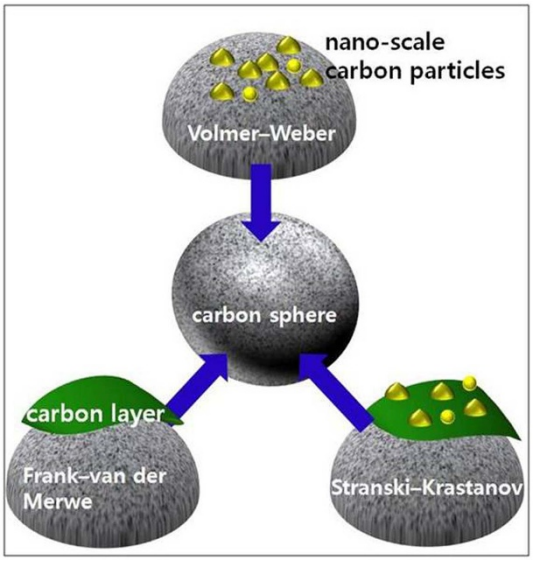

Figure 4 | Schematic drawing of the crystal growth mechanisms on micro-scale SCS. Ostwald ripening was realized by the several growth modes, including the island (Volmer-Weber), the layer-by-layer (Frank-van der Merwe), and the mixed (Stranski-Krastanov) growth modes.

of micro-scale SCSs, and thus small carbon particles form on their surface. Therefore, the overall growth mechanism of micro-scale SCSs is closely associated with Ostwald ripening.

Discussion

The growth modes of micro-scale SCSs. Figure 4 outlines a schematic diagram of the evolution of micro-scale SCSs. Figures 1, 2, and 3 reveal that the surfaces of micro-scale SCSs acts as a substrate for the growth of small carbon particles. In a comparison of flat two-dimensional (2D) substrates, the only difference is that the surface of the micro-scale SCSs has some degree of curvature. According to these observations, the increase in their diameter is clearly related to all of the crystal growth mechanisms, for instance, the layer-by-layer (Frank–van der Merwe), the island (Volmer–Weber), and the mixed (Stranski-Krastanov) growth modes.

The layer-by-layer growth mode usually takes place during homo-epitaxial growth in which the same type of chemical species is attached to the same type of substrate in a low-flux regime. In the evolution of SCSs, the occurrence of the layer-by-layer growth mode is not surprising because large, SCSs become larger by the vapor transport deposition of carbon elements. The island growth mode can be expected when carbon fluxes with higher rates adhere to the surfaces of the growing SCSs because high-rate carbon flux usually causes a deviation from the equilibrium growth state. In this case, heterogeneous nucleation may be prevalent, resulting in the formation of 3D island growth. The third mode, i.e., the mixed mode, can be operated under a carbon flux condition between the two aforementioned extreme cases.

The ostwald ripening process. The growth of micro-scale SCSs through a combination of the island, the layer-by-layer, and the mixed modes was clearly demonstrated on the basis of the observed microstructure evolution. The Ostwald ripening process is the underlying phenomenon occurring in all cases, governing individual atom transfers, and contributing to the evolution to the larger SCSs. Importantly, the three growth modes ubiquitously and simultaneously operate on the growth of SCSs, following the Ostwald ripening process.

Through the Ostwald ripening process, carbon vapors are transferred from other solid carbon sources. Subsequently, the carbon

vapors adsorb onto the sub-micron carbon spheres. Immediately after, the nature of the adsorption of the additional carbon vapors determines the mode, i.e., the island, the layer-by-layer, or the mixed mode. In addition to the microstructure observations, other convincing evidence supporting the operation of Ostwald ripening process is the fact that the carbon structure is disordered in the nano-scale particles but obviously corresponds to the graphite structure in the larger particles, as shown in the SAED pattern (Figure 3).

In summary, we investigated the growth mechanisms of micro-scale SCSs, which were synthesized using GO and a microwave method. Based on observations of the microstructural evolution, we found that Ostwald ripening most likely contributes to their formation. Most importantly, Ostwald ripening was shown in several growth modes, in this case the island, the layer-by-layer, and the mixed growth modes.

Methods

Synthesis of SCSs. Micro-scale SCSs were synthesized using a microwave method. The synthesis procedure of GO was previously reported[26]. GO was synthesized from graphite powder via modification of Hummers and Offeman's method[27]. GO powders in the form of sheets were obtained from the prepared GO suspension through several processes, including centrifugation and heating[26]. The GO sheets were put onto an alumina boat, which was heated in a microwave oven. The microwave oven was purchased from LG electronics Co. Ltd (150 W). Under a constant Ar flow of 60 sccm, the temperature of the microwave oven was increased to 1500°C in 1 min. Annealing was carried out at 1500°C for 3 min at atmospheric pressure. Subsequently, the system was naturally cooled to room temperature under a constant Ar flow rate of 60 sccm. The temperature of the samples was measured by a radiation thermometer (portable digital radiation thermometer, Model No. IR-AHS2, CHINO Co.).

Characterization. The morphology and surface structures of SCSs were examined via SEM (Hitachi S-4200) and TEM (JEOL Ltd., Tokyo, Japan; 200 kV). For TEM, the products were sonicated in acetone for 2 h and centrifuged at 6000 rpm for 10 min. Subsequently, the suspension was dropped on a carbon holey grid and was dried in a vacuum oven at 50°C for 72 h. In order to investigate the chemical composition of CSCs, the EDX pattern was obtained in conjunction with TEM. For examining the crystalline structure of micro-scale SCS and nano-scale particles, SAED patterns were acquired.

1. Bowker, M. The going rate for catalysts. *Nat. Mater.* **1**, 205–206 (2002).
2. Lotty, O. *et al.* Self-seeded growth of germanium nanowires: Coalescence and Ostwald Ripening. *Chem. Mater.* **25**, 215–222 (2013).
3. Granqvist, G. & Buhrman, R. A. Size distributions for supported metal catalysts: Coalescence growth versus ostwald ripening. *J. Catal.* **42**, 477–479 (1976).
4. Fredrick, E., Walstra, P. & Dewettinck, K. Factors gaverning partial coalescence in oil-in-water emulsions. *Adv. Colloid Interf. Sci.* **153**, 30–42 (2010).
5. Yao, J. H., Elder, K. R., Guo, H. & Grant, M. Theory and simulation of Ostwald ripening. *Phy. Rev. B* **47**, 14110–14125 (1993).
6. Voorhees, P. W. The Theory of Ostwald Ripening. *J. Stat. Phys.* **38**, 231–252 (1985).
7. Ostwald, W. Z. Blocking of Ostwald ripening allowing long-term stabilization. *Phys. Chem.* **37**, 385 (1901).
8. Taylor, P. Ostwald ripening in emulsions. *Adv. Colloid Interf. Sci.* **75**, 107–163 (1998).
9. Zhang, J., Huang, F. & Lin, Z. Progress of nanocrystalline growth kinetics based on oriented attachment. *Nanoscale* **2**, 18–34 (2010).
10. Xia, Y. D. & Mokaya, R. Ordered Mesoporous Carbon Hollow Spheres Nanocast Using Mesoporous Silica via Chemical Vapor Deposition. *Adv. Mater.* **16**, 886–891 (2004).
11. Liu, B. Y., Jia, D. C., Meng, Q. C. & Rao, J. C. A novel method for preparation of hollow carbon spheres under a gas pressure atmosphere. *Carbon* **45**, 668–670 (2007).
12. Wang, Y., Su, F. B., Lee, J. Y. & Zhao, X. S. Crystalline Carbon Hollow Spheres, Crystalline Carbon−SnO_2 Hollow Spheres, and Crystalline SnO_2 Hollow Spheres: Synthesis and Performance in Reversible Li-Ion Storage. *Chem. Mater.* **18**, 1347–1353 (2006).
13. Tosheva, L., Parmentier, J., Valtchev, V., Vix-Guterl, C. & Patarin, J. Carbon spheres prepared from zeolite Beta beads. *Carbon* **43**, 2474–2480 (2005).
14. Jin, Y. Z. *et al.* Large-scale synthesis and characterization of carbon spheres prepared by direct pyrolysis of hydrocarbons. *Carbon* **43**, 1944–1953 (2005).
15. Wang, Q., Cao, F. Y., Chen, Q. W. & Chen, C. L. Preparation of carbon micro-spheres by hydrothermal treatment of methylcellulse sol. *Mater. Lett.* **59**, 3738–3741 (2005).
16. Chen, W., Yan, L. & Bangal, P. R. Preparation of graphene by the rapid and mild thermal reduction of graphene oxide induced by microwaves. *Carbon* **48**, 1146–1152 (2010).
17. Rao, K. J., Vaidhyanathan, B., Ganguli, M. & Ramakrishnan, P. A. Synthesis of inorganic solids using microwaves. *Chem. Mater.* **11**, 882–895 (1999).
18. Hu, H., Zhao, Z., Zhou, Q., Gogotsi, Y. & Qiu, J. The role of microwave absorption on formation of graphene from graphite oxide. *Carbon* **50**, 3267–3273 (2012).
19. Liu, X. *et al.* Microwave-assisted synthesis of CdS-reduced graphene oxide composites for photocatalytic reduction of Cr(VI). *Chem. Commun.* **47**, 11984–11986 (2011).
20. Wang, B., Wang, X., Lou, W. & Hao, J. Reduced graphene oxides by microwave-assisted ionothermal treatment. *New J. Chem.* **36**, 1684–1690 (2012).
21. Sakurai, S. *et al.* Role of Subsurface Diffusion and Ostwald Ripening in Catalyst Formation for Single-Walled Carbon Nanotube Forest Growth. *J. Am. Chem. Soc.* **134**, 2148–2153 (2012).
22. Hasegawa, K. & Noda, S. Moderating carbon supply and suppressing Ostwald ripening of catalyst particles to produce 4.5-mm-tall single-walled carbon nanotube forests. *Carbon* **49**, 4497–4504 (2011).
23. Parthasarathy, P. & Virkar, A. V. Electrochemical Ostwald ripening of Pt and Ag catalysts supported on carbon. *J. Power Sources* **234**, 82–90 (2013).
24. Borjesson, A. & Bolton, K. Modeling of Ostwald Ripening of Metal Clusters Attached to Carbon Nanotubes. *J. Phys. Chem. C* **115**, 24454–24462 (2011).
25. Borjesson, A. & Bolton, K. First Principles Studies of the Effect of Ostwald Ripening on Carbon Nanotube Chirality Distributions. *ACS Nano* **5**, 771–779 (2011).
26. Khai, T. V. *et al.* Significant enhancement of blue emission and electrical conductivity of N-doped graphene. *J. Mater. Chem.* **22**, 17992–18003 (2012).
27. Hummers, W. S. Jr. & Offeman, R. E. Preparation of graphitic oxide. *J. Am. Chem. Soc.* **80**, 1339–1339 (1958).

Acknowledgments

This work was supported by the National Research Foundation of Korea (NRF) grant funded by the Korea government (MEST) (no. 2012R1A2A2A01013899).

Author contributions

H.W.K., H.H. and S.S.K. designed the experiments, analyzed the data and prepared the manuscript. H.H. and N.H.P. conducted the experiments. All authors participated in discussion.

Additional information

Supplementary information accompanies this paper at http://www.nature.com/scientificreports

Competing financial interests: The authors declare no competing financial interests.

How to cite this article: Ham, H., Park, N.-H., Kim, S.S. & Kim, H.W. Evidence of Ostwald ripening during evolution of micro-scale solid carbon spheres. *Sci. Rep.* **4**, 3579; DOI:10.1038/srep03579 (2014).